

A New Two-Step Precoding Strategy for Closed-Loop MIMO Systems

Heunchul Lee, *Member, IEEE*, Seokhwan Park, *Student Member, IEEE*,
and Inkyu Lee, *Senior Member, IEEE*

Abstract—In this paper, we present a new precoding technique using rotation transformations for closed loop multiple-input multiple-output (MIMO) wireless systems, which does not require the singular value decomposition (SVD) operation of the channel transfer matrix and allows a simple maximum-likelihood (ML) decoding at the receiver. We divide the precoding process into two steps: orthogonalization transformation which induces orthogonality between transmitted signals and beamforming transformation which achieves diversity gain. In the proposed method, we utilize a design criterion based on the minimum Euclidean distance between the received signals and then the vector orthogonalization is connected to the vector-norm maximization. In this paper, we focus on spatial multiplexing systems transmitting two independent data streams. Compared with the SVD based schemes, the proposed approach maintains a low complexity by relying only on three different kinds of rotation matrices for both the orthogonalization and beamforming transformation. Simulation results confirm that the proposed two step precoding achieves the better performance than the conventional SVD based MIMO precodings with reduced complexity.

Index Terms—Closed-loop systems, maximum likelihood detection (MLD), MIMO systems, space division multiplexing (SDM).

I. INTRODUCTION

MULTIPLE-INPUT MULTIPLE-OUTPUT (MIMO) systems have recently emerged as one of the most significant technical breakthroughs for next generation communication systems. The use of multiple antennas at both transmitter and receiver in wireless communication links has been shown to be capable of achieving extraordinary bit rates without incurring any penalty in power or bandwidth [1] [2]. Expected benefits include higher system capacity and improved quality of service as a result of spatial multiplexing (SM) and diversity

Paper approved by N. Al-Dahir, the Editor for Space-Time, OFDM and Equalization of the IEEE Communications Society. Manuscript received November 16, 2006; revised April 4, 2007, July 22, 2007, and December 5, 2007.

This work was supported in part by the Ministry of Information and Communication (MIC), Korea, under the Information Technology Research Center (ITRC) support program, supervised by the Institute of Information Technology Assessment (IITA), and in part by grant No. R01-2006-000-11112-0 from the Basic Research Program of the Korea Science and Engineering Foundation. This paper was presented in part at the IEEE Vehicular Technology Conference, Calgary, Canada, September 2008.

H. Lee was with the School of Electrical Engineering, Korea University, Seoul 136-702, Korea. He is now with the Department of Electrical Engineering, Stanford University, Stanford, CA 94305 USA (e-mail: heunchul@stanford.edu).

S. Park and I. Lee are with the School of Electrical Engineering, Korea University, Seoul 136-701, Korea (e-mail: shpark@wireless.korea.ac.kr; inkyu@korea.ac.kr).

Digital Object Identifier 10.1109/TCOMM.2009.03.060633

gain [3] [4]. The work in [5] highlights different classes of techniques and algorithms which attempt to realize the various benefits of MIMO systems such as space-time coding schemes.

In open loop systems where channel state information (CSI) is known only at the receiver, the space-time coding techniques exploit transmit diversity [6] [7] [8] while the SM schemes are used to enhance spectral efficiency [9] [10] [11]. Meanwhile, to meet an increasing demand of providing high-rate high-quality multimedia services, we need to obtain a full array gain by utilizing knowledge of the channel at both transmit and receive sides simultaneously. The information theoretic analysis suggests that an additional performance gain can be extracted from multiple antennas in the presence of CSI at the transmitter [12] [13]. In such closed-loop systems, data streams can be transmitted through each eigen mode of the MIMO channel by precoding the input streams prior to transmission [14] [15]. The optimization of linear precoding and decoding has been presented in [16], [17] and [18].

Most work on these closed-loop MIMO systems has been carried out by performing singular value decomposition (SVD) of the channel transfer matrix. It is well known that such SVD-based transmission schemes attain optimality in terms of channel capacity when combined with the water-filling method which allocates the optimized amounts of transmit power to spatial subchannels [2] [15]. Although the SVD-based transmission with waterfilling may be optimal from an information theoretic point of view, it is not necessarily the best scheme in practice because the performance of actual MIMO links is sensitive to other measures such as bit error rate (BER) rather than the maximum mutual information [5]. Moreover, the SVD-based precoding methods may suffer from high computational complexity, since the SVD computation is inherently an iterative process [19]. Therefore, there exists a need to more efficiently perform precoding in a closed-loop MIMO system.

In this paper, we propose a new precoding approach by dividing the precoding process into two steps: orthogonalization transformation which induces orthogonality among transmitted signals and beamforming transformation¹ which achieves diversity gain. We focus on the development of precoding techniques based on three different rotation operations. We will start with a generalization of our earlier works presented in [20] and [21], which introduced the concept of

¹While the term "beamforming" is typically used for the case of single data stream transmission, in this paper the concept of beamforming is extended to general linear precoding.

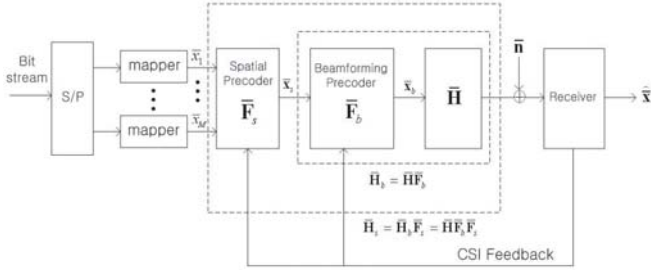


Fig. 1. Schematic diagram of the proposed two-step precoding in closed-loop MIMO systems.

orthogonalized spatial multiplexing (OSM) based on a single rotation transformation. In order to further exploit the diversity gain, we extend the OSM technique in [21] by introducing a new pair of rotation transformations and combining with a beamforming technique presented in [22] and [27]. For optimizing the performance, we use a design criterion based on the minimum Euclidean distance between the received signals [23]. The proposed transmission scheme does not require the SVD operation while a simple maximum-likelihood (ML) decoding is possible at the receiver. Simulation results show that the proposed scheme outperforms the SVD-based schemes with reduced complexity.

For clarity, the following notations are used for the description throughout this paper. Normal letters represent scalar quantities, boldface letters indicate vectors and boldface uppercase letters designate matrices. Letters with a bar account for complex variables. For any complex notation \bar{c} , we denote the real and imaginary part of \bar{c} by $\Re[\bar{c}]$ and $\Im[\bar{c}]$, respectively.

The rest of the paper is organized as follows: In Section II, we present a general description of the proposed two step MIMO precoding algorithm. Section III reviews the OSM algorithm and presents an orthogonalization transformation based on three rotation operations. We also discuss on the criterion for choosing one of the three rotation operations for OSM transmission. Next in Section IV, we describe beamforming transformation which increases the minimum Euclidean distance between different received signal vectors. In Section V, the simulation results are presented comparing the proposed method with other closed-loop MIMO techniques. Finally, the paper is terminated with conclusions in Section VI.

II. SYSTEM DESCRIPTIONS

In this section, we present a general description of the proposed two step MIMO precoding algorithm, as shown in Fig. 1. Consider a MIMO wireless link for flat fading channels with M_t transmit antennas and M_r receive antennas where we transmit M independent data streams simultaneously ($M \leq \min(M_t, M_r)$). The receiver is assumed to have perfect knowledge of the channel.

The proposed MIMO transmission technique applies the two-step precoding process which comprises an orthogonalization precoding, denoted by a matrix $\bar{\mathbf{F}}_s$ of size M -by- M , and a beamforming precoding, denoted by a matrix $\bar{\mathbf{F}}_b$ of size M_t -by- M . At the transmitter, the information bits are first demultiplexed into M parallel substreams and symbol-mapped, which

yields an M -dimensional symbol vector $\bar{\mathbf{x}} = [\bar{x}_1, \dots, \bar{x}_M]^t$ where $(\cdot)^t$ denotes the transpose of a vector or matrix. Here \bar{x}_i is given as $\bar{x}_i = x_{i,I} + jx_{i,Q}$ where $j = \sqrt{-1}$. The orthogonalization precoder $\bar{\mathbf{F}}_s$ receives the symbol vector $\bar{\mathbf{x}}$ and generates an M -dimensional signal vector $\bar{\mathbf{x}}_s = \bar{\mathbf{F}}_s \bar{\mathbf{x}}$. Then the signal vector $\bar{\mathbf{x}}_s$ is further multiplexed by a beamforming precoder $\bar{\mathbf{F}}_b$, which yields an M_t -dimensional symbol vector $\bar{\mathbf{x}}_b = \bar{\mathbf{F}}_b \bar{\mathbf{x}}_s$. The resulting precoded symbol vector $\bar{\mathbf{x}}_b$ is then transmitted from M_t transmit antennas via the MIMO channel $\bar{\mathbf{H}}$ to the receiver.

Let us define the M_r -dimensional complex received signal vector $\bar{\mathbf{y}}$ as

$$\bar{\mathbf{y}} = \bar{\mathbf{H}} \bar{\mathbf{F}}_b \bar{\mathbf{F}}_s \bar{\mathbf{x}} + \bar{\mathbf{n}} \quad (1)$$

where $\bar{\mathbf{n}}$ is a complex Gaussian noise vector with the covariance matrix $\sigma_n^2 \mathbf{I}_{M_r}$. Here \mathbf{I}_d indicates an identity matrix of size d . In (1), the channel response matrix can be written as

$$\bar{\mathbf{H}} = [\bar{\mathbf{h}}_1 \ \bar{\mathbf{h}}_2 \ \dots \ \bar{\mathbf{h}}_{M_t}] = \begin{bmatrix} \bar{h}_{11} & \dots & \bar{h}_{1M_t} \\ \vdots & \ddots & \vdots \\ \bar{h}_{M_r 1} & \dots & \bar{h}_{M_r M_t} \end{bmatrix}$$

where $\bar{\mathbf{h}}_i$ denotes the i -th column of $\bar{\mathbf{H}}$ and \bar{h}_{ji} represents the channel response coefficient between the i th transmit and the j th receive antenna. At the receiver, the ML receiver provides the estimated symbol vector $\hat{\bar{\mathbf{x}}} = [\hat{\bar{x}}_1, \dots, \hat{\bar{x}}_M]^t$, which is an ML estimate of the transmitted symbol vector $\bar{\mathbf{x}} = [\bar{x}_1, \dots, \bar{x}_M]^t$.

In the following definition, we shall define three different kinds of orthogonality between two complex-valued vectors [22].

Definition 1: For two complex vectors $\bar{\mathbf{v}}_1$ and $\bar{\mathbf{v}}_2$, the Hermitian product is defined by

$$\begin{aligned} \langle \bar{\mathbf{v}}_1, \bar{\mathbf{v}}_2 \rangle &= \bar{\mathbf{v}}_1^\dagger \bar{\mathbf{v}}_2 \\ &= \langle \bar{\mathbf{v}}_1, \bar{\mathbf{v}}_2 \rangle_R + j \langle \bar{\mathbf{v}}_1, \bar{\mathbf{v}}_2 \rangle_I \end{aligned}$$

where $\langle \bar{\mathbf{v}}_1, \bar{\mathbf{v}}_2 \rangle_R$ and $\langle \bar{\mathbf{v}}_1, \bar{\mathbf{v}}_2 \rangle_I$ indicate the real part and the imaginary part of $\langle \bar{\mathbf{v}}_1, \bar{\mathbf{v}}_2 \rangle$, respectively, and $(\cdot)^\dagger$ denotes the complex conjugate transpose of a vector or matrix. Here $\bar{\mathbf{v}}_1$ and $\bar{\mathbf{v}}_2$ are said to be *inner orthogonal* if $\langle \bar{\mathbf{v}}_1, \bar{\mathbf{v}}_2 \rangle_R = 0$. Similarly, *outer orthogonal* is defined if $\langle \bar{\mathbf{v}}_1, \bar{\mathbf{v}}_2 \rangle_I = 0$. Note that in general we refer to two complex vectors $\bar{\mathbf{v}}_1$ and $\bar{\mathbf{v}}_2$ as being *complex orthogonal* if and only if they are both inner and outer orthogonal.

Now we briefly discuss the connection between the vector-norm maximization and the vector orthogonalization process. For example, given two M_r -dimensional complex vectors $\bar{\mathbf{v}}_1$ and $\bar{\mathbf{v}}_2$, we consider a unitary transformation $\bar{\mathbf{P}}_o$ which maximizes $\|\bar{\mathbf{v}}_1'\|$ and minimizes $\|\bar{\mathbf{v}}_2'\|$ as

$$[\bar{\mathbf{v}}_1' \ \bar{\mathbf{v}}_2'] = [\bar{\mathbf{v}}_1 \ \bar{\mathbf{v}}_2] \bar{\mathbf{P}}_o, \quad (2)$$

where $\|\cdot\|$ denotes the Euclidean norm. Utilizing the SVD of the M_r -by-two matrix $[\bar{\mathbf{v}}_1 \ \bar{\mathbf{v}}_2]$ in (2), we can represent the matrix $[\bar{\mathbf{v}}_1' \ \bar{\mathbf{v}}_2']$ as

$$[\bar{\mathbf{v}}_1' \ \bar{\mathbf{v}}_2'] = [\bar{\mathbf{u}}_1 \ \bar{\mathbf{u}}_2] \begin{bmatrix} \lambda_{max} & 0 \\ 0 & \lambda_{min} \end{bmatrix} [\bar{\mathbf{w}}_1 \ \bar{\mathbf{w}}_2]^\dagger$$

where $\{\bar{\mathbf{u}}_1, \bar{\mathbf{u}}_2\}$ and $\{\bar{\mathbf{w}}_1, \bar{\mathbf{w}}_2\}$ are the two left and right singular vectors corresponding to non-zero singular values

λ_{max} and λ_{min} , respectively. This trimmed-down version of the SVD is referred to as the *thin* SVD [19]. Then, it is clear from the definition of the SVD that if the right singular vectors $[\bar{\mathbf{w}}_1 \ \bar{\mathbf{w}}_2]$ are employed as $\bar{\mathbf{P}}_o$ in (2), the norm of $\bar{\mathbf{v}}'_1$ reaches its maximum value of λ_{max} [24] since

$$\begin{aligned} [\bar{\mathbf{v}}'_1 \ \bar{\mathbf{v}}'_2] &= [\bar{\mathbf{u}}_1 \ \bar{\mathbf{u}}_2] \begin{bmatrix} \lambda_{max} & 0 \\ 0 & \lambda_{min} \end{bmatrix} [\bar{\mathbf{w}}_1 \ \bar{\mathbf{w}}_2]^\dagger [\bar{\mathbf{w}}_1 \ \bar{\mathbf{w}}_2] \\ &= [\lambda_{max} \bar{\mathbf{u}}_1 \ \lambda_{min} \bar{\mathbf{u}}_2]. \end{aligned}$$

Meanwhile, the norm of the other column $\bar{\mathbf{v}}'_2$ is minimized as λ_{min} . It should be noted that $(\bar{\mathbf{v}}'_1)^\dagger \bar{\mathbf{v}}'_2 = 0$ even though $\bar{\mathbf{v}}_1$ and $\bar{\mathbf{v}}_2$ may not be orthogonal. This complex orthogonalization of two column vectors $\bar{\mathbf{v}}'_1$ and $\bar{\mathbf{v}}'_2$ results from the first order condition for the maximum of $\|\bar{\mathbf{v}}'_1\|$ [25].

In this paper, we will utilize the connection of the vector orthogonalization with the vector-norm maximization to describe our new precoding technique. In particular, in Section III we will apply the orthogonality relation to the design of $\bar{\mathbf{F}}_s$ while exploiting the aspect of the norm maximization in the design of $\bar{\mathbf{F}}_b$ in Section IV.

III. ORTHOGONALIZATION TRANSFORMATION FOR OSM

In this section, we review the OSM scheme introduced in [21] and present the orthogonality precoder $\bar{\mathbf{F}}_s$ by introducing new rotation matrices presented in [22] and [27]. These rotation matrices will also be employed for development of $\bar{\mathbf{F}}_b$ in Section IV.

As shown in Fig. 1, we apply the beamforming transformation $\bar{\mathbf{F}}_b$ on the original channel response matrix $\bar{\mathbf{H}}$ to obtain $\bar{\mathbf{H}}_b$, which is further transformed into the effective channel matrix $\bar{\mathbf{H}}_s$ by the orthogonalization transformation $\bar{\mathbf{F}}_s$ (i.e., $\bar{\mathbf{H}}_s = \bar{\mathbf{H}}_b \bar{\mathbf{F}}_s = \bar{\mathbf{H}} \bar{\mathbf{F}}_b \bar{\mathbf{F}}_s$). The beamforming transformation $\bar{\mathbf{F}}_b$ will be described in detail in the following section. For now, we assume that a beamforming matrix $\bar{\mathbf{F}}_b$ is given. In this section, we present an orthogonalization transformation $\bar{\mathbf{F}}_s$ based on three different kinds of rotation matrices for OSM transmission and describe the corresponding ML decoding method by converting the complex signal model into a real lattice notation, which allows a simple ML decoding at the receiver. Our interest is restricted to spatial multiplexing systems transmitting two independent data streams (i.e., $M = 2$), which are important in practical wireless system designs.

Now we can write the transmitted signal vectors as $\bar{\mathbf{x}} = [\bar{x}_1 \ \bar{x}_2]^t$. For an M_c -ary QAM modulation system, the real-valued symbols $x_{i,I}$ and $x_{i,Q}$ are chosen from a PAM signal set $\mathcal{S}_\eta = \pm 1, \pm 3, \dots, \pm(2^{\frac{\eta}{2}} - 1)$, where $\eta = \log_2 M_c$ denotes the number of bits per symbol (two dimensions).

By defining $\bar{\mathbf{H}}_b = \begin{bmatrix} \bar{\mathbf{h}}_1^b & \bar{\mathbf{h}}_2^b \end{bmatrix} = \bar{\mathbf{H}} \bar{\mathbf{F}}_b$ and $\bar{\mathbf{H}}_s = \begin{bmatrix} \bar{\mathbf{h}}_1^s & \bar{\mathbf{h}}_2^s \end{bmatrix} = \bar{\mathbf{H}}_b \bar{\mathbf{F}}_s$, the original system model in (1) can be written as

$$\begin{aligned} \bar{\mathbf{y}} &= \bar{\mathbf{H}}_b \bar{\mathbf{F}}_s \bar{\mathbf{x}} + \bar{\mathbf{n}} \\ &= \bar{\mathbf{H}}_s \bar{\mathbf{x}} + \bar{\mathbf{n}} \end{aligned} \quad (3)$$

where the M_r -by-two matrix $\bar{\mathbf{H}}_b$ accounts for the effective channel matrix for $\bar{\mathbf{x}}_s = \bar{\mathbf{F}}_s \bar{\mathbf{x}}$.

Equivalently, the real-valued representation of the system (3) is given as [26]

$$\mathbf{y} = \mathbf{H}_b \mathbf{F}_s \mathbf{x} + \mathbf{n} = \mathbf{H}_s \mathbf{x} + \mathbf{n}$$

where $\mathbf{y} = [\Re[\bar{\mathbf{y}}^t] \ \Im[\bar{\mathbf{y}}^t]]^t$, $\mathbf{x} = [\Re[\bar{\mathbf{x}}^t] \ \Im[\bar{\mathbf{x}}^t]]^t = [x_{1,I} \ x_{2,I} \ x_{1,Q} \ x_{2,Q}]^t$, $\mathbf{n} = [\Re[\bar{\mathbf{n}}^t] \ \Im[\bar{\mathbf{n}}^t]]^t$, $\mathbf{F}_s = \begin{bmatrix} \Re[\bar{\mathbf{F}}_s] & -\Im[\bar{\mathbf{F}}_s] \\ \Im[\bar{\mathbf{F}}_s] & \Re[\bar{\mathbf{F}}_s] \end{bmatrix}$, $\mathbf{H}_b = \begin{bmatrix} \Re[\bar{\mathbf{H}}_b] & -\Im[\bar{\mathbf{H}}_b] \\ \Im[\bar{\mathbf{H}}_b] & \Re[\bar{\mathbf{H}}_b] \end{bmatrix} = \begin{bmatrix} \mathbf{h}_1^b & \mathbf{h}_2^b & \dot{\mathbf{h}}_1^b & \dot{\mathbf{h}}_2^b \end{bmatrix}$, and

$$\mathbf{H}_s = \mathbf{H}_b \mathbf{F}_s = \begin{bmatrix} \Re[\bar{\mathbf{H}}_s] & -\Im[\bar{\mathbf{H}}_s] \\ \Im[\bar{\mathbf{H}}_s] & \Re[\bar{\mathbf{H}}_s] \end{bmatrix} = \begin{bmatrix} \mathbf{h}_1^s & \mathbf{h}_2^s & \dot{\mathbf{h}}_1^s & \dot{\mathbf{h}}_2^s \end{bmatrix}. \quad (4)$$

Here \mathbf{n} is a real Gaussian noise vector with the covariance matrix $\frac{\sigma_n^2}{2} \mathbf{I}_{2M_r}$.

We notice that from the definition of the real-valued representation in (4), the column vectors \mathbf{h}_1^s and \mathbf{h}_2^s are orthogonal to $\dot{\mathbf{h}}_1^s$ and $\dot{\mathbf{h}}_2^s$, respectively, regardless of \mathbf{F}_s . Furthermore, it is easy to show that $\|\mathbf{h}_1^s\| = \|\dot{\mathbf{h}}_1^s\|$ and $\|\mathbf{h}_2^s\| = \|\dot{\mathbf{h}}_2^s\|$.

Based on this lattice representation, the ML estimate of the transmitted vector \mathbf{x} is obtained by

$$\begin{aligned} \hat{\mathbf{x}} &= [\hat{x}_{1,I}, \hat{x}_{2,I}, \hat{x}_{1,Q}, \hat{x}_{2,Q}]^t \\ &= \arg \min_{x_{1,I}, x_{2,I}, x_{1,Q}, x_{2,Q} \in \mathcal{S}_\eta} \|\mathbf{y} - \mathbf{H}_s \mathbf{x}\|^2. \end{aligned} \quad (5)$$

Note that the ML decoding complexity in this case is polynomial in the number of constellation points.

In what follows, we present a precoding matrix \mathbf{F}_s that achieves orthogonality between columns of \mathbf{H}_s in (4), which allows a simple ML decoding in (5). From Definition 1 and Equation (4), we obtain the following relations:

$$\langle \bar{\mathbf{h}}_1^s, \bar{\mathbf{h}}_2^s \rangle_R = \mathbf{h}_1^s \cdot \mathbf{h}_2^s = \dot{\mathbf{h}}_1^s \cdot \dot{\mathbf{h}}_2^s \quad (6)$$

and

$$\langle \bar{\mathbf{h}}_1^s, \bar{\mathbf{h}}_2^s \rangle_I = \mathbf{h}_1^s \cdot \dot{\mathbf{h}}_2^s = -\mathbf{h}_2^s \cdot \dot{\mathbf{h}}_1^s \quad (7)$$

where \cdot denotes the inner (dot) product between two real-valued vectors. These properties are essential to the development of the proposed scheme.

We first review the OSM scheme proposed in [21], where the following rotation matrix $\bar{\mathbf{S}}(\theta)$ is employed for $\bar{\mathbf{F}}_s$ as

$$\bar{\mathbf{S}}(\theta) = \begin{bmatrix} 1 & 0 \\ 0 & \exp(j\theta) \end{bmatrix}.$$

We will refer to this scheme as *original* mode. In the real-valued representation, the corresponding rotation operation can be written as

$$\mathbf{S}(\theta) = \begin{bmatrix} \Re[\bar{\mathbf{S}}(\theta)] & -\Im[\bar{\mathbf{S}}(\theta)] \\ \Im[\bar{\mathbf{S}}(\theta)] & \Re[\bar{\mathbf{S}}(\theta)] \end{bmatrix} = \begin{bmatrix} 1 & 0 & 0 & 0 \\ 0 & \cos(\theta) & 0 & -\sin(\theta) \\ 0 & 0 & 1 & 0 \\ 0 & \sin(\theta) & 0 & \cos(\theta) \end{bmatrix}.$$

It is shown in [21] that by applying the rotation angle

$$\theta_S = \tan^{-1} \left(\frac{\langle \bar{\mathbf{h}}_1^b, \bar{\mathbf{h}}_2^b \rangle_I}{\langle \bar{\mathbf{h}}_1^b, \bar{\mathbf{h}}_2^b \rangle_R} \right),$$

we can write the effective channel matrix in (4) for the original mode as

$$\begin{aligned} \mathbf{H}_s &= \begin{bmatrix} \mathbf{h}_1^s & \mathbf{h}_2^s & \dot{\mathbf{h}}_1^s & \dot{\mathbf{h}}_2^s \end{bmatrix} \\ &= \begin{bmatrix} \mathbf{h}_1^b & \mathbf{h}_2^b & \dot{\mathbf{h}}_1^b & \dot{\mathbf{h}}_2^b \end{bmatrix} \begin{bmatrix} 1 & 0 & 0 & 0 \\ 0 & \cos(\theta_S) & 0 & -\sin(\theta_S) \\ 0 & 0 & 1 & 0 \\ 0 & \sin(\theta_S) & 0 & \cos(\theta_S) \end{bmatrix} \end{aligned}$$

where now we have the relations $\mathbf{h}_1^s \perp \mathbf{h}_2^s$ and $\mathbf{h}_2^s \perp \mathbf{h}_1^s$ as well as $\mathbf{h}_1^s \perp \mathbf{h}_1^s$ and $\mathbf{h}_2^s \perp \mathbf{h}_2^s$.

Therefore, for the original OSM with $\overline{\mathbf{F}}_s = \overline{\mathbf{S}}(\theta_s)$, the resulting two vectors $\overline{\mathbf{h}}_1^s$ and $\overline{\mathbf{h}}_2^s$ become outer orthogonal since $\langle \overline{\mathbf{h}}_1^s, \overline{\mathbf{h}}_2^s \rangle_I = \mathbf{h}_1^s \cdot \mathbf{h}_2^s = \mathbf{h}_2^s \cdot \mathbf{h}_1^s = 0$, but $\langle \overline{\mathbf{h}}_1^s, \overline{\mathbf{h}}_2^s \rangle_R \neq 0$. What is more important to note is that the subspace spanned by \mathbf{h}_1^s and \mathbf{h}_2^s is orthogonal to that spanned by \mathbf{h}_1^s and \mathbf{h}_2^s . Utilizing the established orthogonality between the columns of \mathbf{H}_s , the ML solution $\hat{\mathbf{x}} = [\hat{x}_1 \hat{x}_2]^t$ in Equation (5) for the original OSM can be individually given by [21]

$$[\hat{x}_{1,I} \hat{x}_{2,I}] = \arg \min_{x_{1,I}, x_{2,I} \in \mathcal{S}_\eta} \left\| \mathbf{y} - [\mathbf{h}_1^s \mathbf{h}_2^s] \begin{bmatrix} x_{1,I} \\ x_{2,I} \end{bmatrix} \right\|^2 \quad (8)$$

and

$$[\hat{x}_{1,Q} \hat{x}_{2,Q}] = \arg \min_{x_{1,Q}, x_{2,Q} \in \mathcal{S}_\eta} \left\| \mathbf{y} - [\mathbf{h}_1^s \mathbf{h}_2^s] \begin{bmatrix} x_{1,Q} \\ x_{2,Q} \end{bmatrix} \right\|^2. \quad (9)$$

Note that the size of the search set for each metric reduces from M_c^2 to M_c compared to (5). In other words, the complexity of the ML decoding of the proposed system is the same as symbol-by-symbol decoding.

Next, we introduce two other new rotation matrices for OSM using the method in [22]. We first derive a precoding matrix \mathbf{F}_s which establishes the inner orthogonality between $\overline{\mathbf{h}}_1^s$ and $\overline{\mathbf{h}}_2^s$ ($\langle \overline{\mathbf{h}}_1^s, \overline{\mathbf{h}}_2^s \rangle_R = 0$). From Equation (6), it is obvious that in order to establish the inner orthogonality, we need to achieve the orthogonality $\mathbf{h}_1^s \perp \mathbf{h}_2^s$ and $\mathbf{h}_1^s \perp \mathbf{h}_1^s$. To this end, we can apply the following transformation

$$\mathbf{H}_s = \begin{bmatrix} \mathbf{h}_1^s & \mathbf{h}_2^s & \mathbf{h}_1^s & \mathbf{h}_2^s \end{bmatrix} = \begin{bmatrix} \mathbf{h}_1^b & \mathbf{h}_2^b & \mathbf{h}_1^b & \mathbf{h}_2^b \end{bmatrix} \times \begin{bmatrix} \cos(\theta) & \sin(\theta) & 0 & 0 \\ -\sin(\theta) & \cos(\theta) & 0 & 0 \\ 0 & 0 & \cos(\theta) & \sin(\theta) \\ 0 & 0 & -\sin(\theta) & \cos(\theta) \end{bmatrix} \quad (10)$$

which is equivalent to, in a complex domain,

$$[\overline{\mathbf{h}}_1^s \ \overline{\mathbf{h}}_2^s] = [\overline{\mathbf{h}}_1^b \ \overline{\mathbf{h}}_2^b] \overline{\mathbf{I}}(\theta) \quad (11)$$

where the *inner* rotation matrix $\overline{\mathbf{I}}(\theta)$ is given as (a.k.a., *Givens rotations* [19])

$$\overline{\mathbf{I}}(\theta) = \begin{bmatrix} \cos(\theta) & \sin(\theta) \\ -\sin(\theta) & \cos(\theta) \end{bmatrix}.$$

This OSM mode will be referred to as *inner* mode.

From Equation (10), we can establish the inner orthogonality if

$$\begin{aligned} \langle \overline{\mathbf{h}}_1^s, \overline{\mathbf{h}}_2^s \rangle_R &= \mathbf{h}_1^s \cdot \mathbf{h}_2^s = \left(\|\overline{\mathbf{h}}_1^b\|^2 - \|\overline{\mathbf{h}}_2^b\|^2 \right) \cos \theta \sin \theta \\ &+ ((\cos \theta)^2 - (\sin \theta)^2) \langle \overline{\mathbf{h}}_1^b, \overline{\mathbf{h}}_2^b \rangle_R = 0. \end{aligned}$$

Then, after some manipulations, the optimal rotation angle results in

$$\theta_I = \text{Atan} \left(\left(\|\overline{\mathbf{h}}_1^b\|^2 - \|\overline{\mathbf{h}}_2^b\|^2, \langle \overline{\mathbf{h}}_1^b, \overline{\mathbf{h}}_2^b \rangle_R \right) \right)$$

$$\text{where } \text{Atan}(x, y) \triangleq \tan^{-1} \left(\frac{x - \sqrt{x^2 + 4y^2}}{2y} \right).$$

With this inner orthogonality, we achieve $\mathbf{h}_1^s \perp \mathbf{h}_2^s$ and $\mathbf{h}_1^s \perp \mathbf{h}_1^s$ as well as $\mathbf{h}_2^s \perp \mathbf{h}_1^s$ and $\mathbf{h}_2^s \perp \mathbf{h}_2^s$, which means that the subspace spanned by \mathbf{h}_1^s and \mathbf{h}_2^s is orthogonal to that spanned by \mathbf{h}_1^s and \mathbf{h}_2^s . It follows that the ML solution $\hat{\mathbf{x}}$ in Equation (5) for the inner OSM can be obtained by

$$[\hat{x}_{1,I} \hat{x}_{2,Q}] = \arg \min_{x_{1,I}, x_{2,Q} \in \mathcal{S}_\eta} \left\| \mathbf{y} - [\mathbf{h}_1^s \ \mathbf{h}_2^s] \begin{bmatrix} x_{1,I} \\ x_{2,Q} \end{bmatrix} \right\|^2$$

and

$$[\hat{x}_{2,I} \hat{x}_{1,Q}] = \arg \min_{x_{2,I}, x_{1,Q} \in \mathcal{S}_\eta} \left\| \mathbf{y} - [\mathbf{h}_2^s \ \mathbf{h}_1^s] \begin{bmatrix} x_{2,I} \\ x_{1,Q} \end{bmatrix} \right\|^2.$$

Finally, we consider a rotation matrix for the OSM based on the outer orthogonality ($\langle \overline{\mathbf{h}}_1^s, \overline{\mathbf{h}}_2^s \rangle_I = 0$). From Equation (7), in order to make the two column vectors $\overline{\mathbf{h}}_1^s$ and $\overline{\mathbf{h}}_2^s$ become outer orthogonal, we need to apply a rotation transformation onto a pair of columns $\{\mathbf{h}_1^b, \mathbf{h}_2^b\}$ and $\{\mathbf{h}_2^b, \mathbf{h}_1^b\}$ in (4) so that $\mathbf{h}_1^s \perp \mathbf{h}_2^s$ and $\mathbf{h}_2^s \perp \mathbf{h}_1^s$. The corresponding rotation operation can be written as

$$\begin{bmatrix} \mathbf{h}_1^s & \mathbf{h}_2^s & \mathbf{h}_1^s & \mathbf{h}_2^s \end{bmatrix} = \begin{bmatrix} \mathbf{h}_1^b & \mathbf{h}_2^b & \mathbf{h}_1^b & \mathbf{h}_2^b \end{bmatrix} \times \begin{bmatrix} \cos(\theta) & 0 & 0 & -\sin(\theta) \\ 0 & \cos(\theta) & -\sin(\theta) & 0 \\ 0 & \sin(\theta) & \cos(\theta) & 0 \\ \sin(\theta) & 0 & 0 & \cos(\theta) \end{bmatrix}$$

which is equivalent to

$$[\overline{\mathbf{h}}_1^s \ \overline{\mathbf{h}}_2^s] = [\overline{\mathbf{h}}_1^b \ \overline{\mathbf{h}}_2^b] \overline{\mathbf{O}}(\theta) \quad (12)$$

where the *outer* rotation matrix $\overline{\mathbf{O}}(\theta)$ is defined as

$$\overline{\mathbf{O}}(\theta) = \begin{bmatrix} \cos(\theta) & j \sin(\theta) \\ j \sin(\theta) & \cos(\theta) \end{bmatrix}.$$

This OSM mode will be referred to as *outer* mode.

In this case, we can achieve the outer orthogonality between $\overline{\mathbf{h}}_1^s$ and $\overline{\mathbf{h}}_2^s$ by applying the following rotation angle

$$\theta_O = \text{Atan} \left(\left(\|\overline{\mathbf{h}}_1^b\|^2 - \|\overline{\mathbf{h}}_2^b\|^2, \langle \overline{\mathbf{h}}_1^b, \overline{\mathbf{h}}_2^b \rangle_I \right) \right).$$

In the *outer* mode, the outer orthogonality guarantees that we can use the same ML decoding metric of (8) and (9) as in the original mode.

Now we have three different OSM modes for $\overline{\mathbf{F}}_s$. Thus, we need to select the best mode among the three modes for each channel realization. We will present a selection metric based on the minimum Euclidean distance since the minimum Euclidean distance between the received signals for two transmitted signals $\overline{\mathbf{x}}_c = [\overline{x}_{1,c} \ \overline{x}_{2,c}]^t$ and $\overline{\mathbf{x}}_e = [\overline{x}_{1,e} \ \overline{x}_{2,e}]^t$ ($\overline{\mathbf{x}}_c \neq \overline{\mathbf{x}}_e$) accounts for the performance of the ML receiver at high signal-to-noise ratio (SNR) [23].

Given the effective channel $\overline{\mathbf{H}}_b = [\overline{\mathbf{h}}_1^b \ \overline{\mathbf{h}}_2^b]$, we can compute the squared minimum distance $d_{min}^2(\overline{\mathbf{H}}_b, \overline{\mathbf{F}}_s)$ as

$$\begin{aligned} d_{min}^2(\overline{\mathbf{H}}_b, \overline{\mathbf{F}}_s) &= \min_{\overline{\mathbf{x}}_c, \overline{\mathbf{x}}_e \in \mathcal{Q}^2} \left\| \overline{\mathbf{H}}_s(\overline{\mathbf{x}}_c - \overline{\mathbf{x}}_e) \right\|^2 \\ &= \min_{\overline{\mathbf{x}}_c, \overline{\mathbf{x}}_e \in \mathcal{Q}^2} \left\| [\mathbf{h}_1^s \ \mathbf{h}_2^s \ \mathbf{h}_1^s \ \mathbf{h}_2^s] \begin{bmatrix} \Re[\overline{x}_{1,c} - \overline{x}_{1,e}] \\ \Re[\overline{x}_{2,c} - \overline{x}_{2,e}] \\ \Im[\overline{x}_{1,c} - \overline{x}_{1,e}] \\ \Im[\overline{x}_{2,c} - \overline{x}_{2,e}] \end{bmatrix} \right\|^2 \end{aligned} \quad (13)$$

where Q denotes a QAM constellation of size M_c .

Note again that in the case of the OSM transmission with original or outer mode the outer orthogonality makes the subspace spanned by \mathbf{h}_1^s and \mathbf{h}_2^s orthogonal to that spanned by \mathbf{h}_1^s and \mathbf{h}_2^s . Furthermore, we notice that the geometrical relationship between \mathbf{h}_1^s and \mathbf{h}_2^s remains the same as that between $\hat{\mathbf{h}}_1^s$ and $\hat{\mathbf{h}}_2^s$ since the lengths of two vectors \mathbf{h}_1^s and \mathbf{h}_2^s and the angle between them are the same as $\hat{\mathbf{h}}_1^s$ and $\hat{\mathbf{h}}_2^s$'s (i.e., $\|\mathbf{h}_1^s\| = \|\hat{\mathbf{h}}_1^s\|$, $\|\mathbf{h}_2^s\| = \|\hat{\mathbf{h}}_2^s\|$, and $\mathbf{h}_1^s \cdot \mathbf{h}_2^s = \hat{\mathbf{h}}_1^s \cdot \hat{\mathbf{h}}_2^s$). This property indicates that two pairs of real signals $\{x_{1,I}, x_{2,I}\}$ and $\{x_{1,Q}, x_{2,Q}\}$ in (8) and (9) experience effective channels with the same quality with respect to the minimum Euclidean distance. In other words, when computing the minimum distance, we need to consider only one of the two subspaces. In this case, assuming that two symbols \bar{x}_1 and \bar{x}_2 employ the same constellation, for both the original and outer modes, i.e., $\bar{\mathbf{F}}_s = \bar{\mathbf{O}}(\theta_O)$ or $\bar{\mathbf{S}}(\theta_S)$, Equation (13) can be simplified as [21]

$$d_{min}^2(\bar{\mathbf{H}}_b, \bar{\mathbf{F}}_s) = \min_{x_{1,I}^c, x_{1,I}^e, x_{2,I}^c, x_{2,I}^e \in \mathcal{S}_\eta} \left\| \begin{bmatrix} \mathbf{h}_1^s & \mathbf{h}_2^s \end{bmatrix} \begin{bmatrix} x_{1,I}^c - x_{1,I}^e \\ x_{2,I}^c - x_{2,I}^e \end{bmatrix} \right\|^2, \quad (14)$$

where we define $x_{1,I}^c = \Re[\bar{x}_{1,c}]$, $x_{1,I}^e = \Re[\bar{x}_{1,e}]$, $x_{2,I}^c = \Re[\bar{x}_{2,c}]$, and $x_{2,I}^e = \Re[\bar{x}_{2,e}]$.

In a similar way, we can obtain the minimum Euclidean distance for the inner OSM mode as

$$d_{min}^2(\bar{\mathbf{H}}_b, \bar{\mathbf{I}}(\theta_I)) = \min_{x_{1,I}^c, x_{1,I}^e, x_{2,Q}^c, x_{2,Q}^e \in \mathcal{S}_\eta} \left\| \begin{bmatrix} \mathbf{h}_1^s & \hat{\mathbf{h}}_2^s \end{bmatrix} \begin{bmatrix} x_{1,I}^c - x_{1,I}^e \\ x_{2,Q}^c - x_{2,Q}^e \end{bmatrix} \right\|^2 \quad (15)$$

where $x_{2,Q}^c = \Im[\bar{x}_{2,c}]$ and $x_{2,Q}^e = \Im[\bar{x}_{2,e}]$.

Now we are ready to present a selection criterion based on the minimum Euclidean distance. Let $\bar{\mathbf{F}}_s^*$ be an optimal mode for a given channel realization selected from the set of rotation matrices $\mathcal{F}_U = \{\bar{\mathbf{S}}(\theta_S), \bar{\mathbf{I}}(\theta_I), \bar{\mathbf{O}}(\theta_O)\}$. Then, we can determine the optimal mode by choosing $\bar{\mathbf{F}}_s^*$ which has the largest minimum Euclidean distance as

$$\bar{\mathbf{F}}_s^* = \arg \max_{\bar{\mathbf{F}}_s \in \mathcal{F}_U} d_{min}^2(\bar{\mathbf{H}}_b, \bar{\mathbf{F}}_s). \quad (16)$$

It follows from the equation above that the achievable minimum Euclidean distance for a given channel matrix $\bar{\mathbf{H}}_b$ is denoted by $d_{min}^2(\bar{\mathbf{H}}_b, \bar{\mathbf{F}}_s^*)$. In the simulation section, we will show that we can achieve a significant performance gain by appropriately choosing the OSM mode based on the above selection criterion for each channel realization. In the following section, we will illustrate a beamforming transformation $\bar{\mathbf{F}}_b$ based on the maximization of $d_{min}^2(\bar{\mathbf{H}}_b, \bar{\mathbf{F}}_s^*)$.

IV. BEAMFORMING TRANSFORMATION FOR INCREASING THE EUCLIDEAN DISTANCE

In this section, we study a beamforming transformation $\bar{\mathbf{F}}_b$ to apply the OSM transmission to MIMO systems with more than two transmit antennas ($M_t > 2$). In the two transmit antenna case, $\bar{\mathbf{F}}_s$ can be employed alone without $\bar{\mathbf{F}}_b$. While in the previous section the rotation matrices are used to establish the inner and outer orthogonality between two channel column

vectors, in this section we employ the inner and outer rotation matrices in the design of $\bar{\mathbf{F}}_b$ to exploit the aspect of the norm maximization.

We first define two M_t -by- M_t rotation matrices: the inner rotation matrix $\bar{\mathbf{I}}(i, j, \bar{\mathbf{H}})$ and the outer rotation matrix $\bar{\mathbf{O}}(i, j, \bar{\mathbf{H}})$, as an extension of two-by-two matrices $\bar{\mathbf{I}}(\theta_I)$ and $\bar{\mathbf{O}}(\theta_O)$. The inner rotation matrix $\bar{\mathbf{I}}(i, j, \bar{\mathbf{H}})$ with an index pair (i, j) and the channel matrix $\bar{\mathbf{H}}$ has the form of

$$\bar{\mathbf{I}}(i, j, \bar{\mathbf{H}}) = \begin{bmatrix} 1 & \cdots & 0 & \cdots & 0 & \cdots & 0 \\ \vdots & \ddots & \vdots & & \vdots & & \vdots \\ 0 & \cdots & \cos(\theta_I^{ij}) & \cdots & \sin(\theta_I^{ij}) & \cdots & 0 \\ \vdots & & \vdots & \ddots & \vdots & & \vdots \\ 0 & \cdots & -\sin(\theta_I^{ij}) & \cdots & \cos(\theta_I^{ij}) & \cdots & 0 \\ \vdots & & \vdots & & \vdots & \ddots & \vdots \\ 0 & \cdots & 0 & \cdots & 0 & \cdots & 1 \end{bmatrix}$$

where

$$\theta_I^{ij} = \text{Atan}(\|\bar{\mathbf{h}}_i\|^2 - \|\bar{\mathbf{h}}_j\|^2, \langle \bar{\mathbf{h}}_i, \bar{\mathbf{h}}_j \rangle_R).$$

Here $\bar{\mathbf{I}}(i, j, \bar{\mathbf{H}})$ is an identity matrix with the exception of $[\bar{\mathbf{I}}(i, j, \bar{\mathbf{H}})]_{i,i} = \cos(\theta_I^{ij})$, $[\bar{\mathbf{I}}(i, j, \bar{\mathbf{H}})]_{i,j} = \sin(\theta_I^{ij})$, $[\bar{\mathbf{I}}(i, j, \bar{\mathbf{H}})]_{j,i} = -\sin(\theta_I^{ij})$ and $[\bar{\mathbf{I}}(i, j, \bar{\mathbf{H}})]_{j,j} = \cos(\theta_I^{ij})$, where $[\cdot]_{m,n}$ denotes the (m, n) -th element of a matrix.

In a similar way, the outer rotation matrix $\bar{\mathbf{O}}(i, j, \bar{\mathbf{H}})$ is given by the identity matrix of size M_t with the exception of $[\bar{\mathbf{O}}(i, j, \bar{\mathbf{H}})]_{i,i} = \cos(\theta_O^{ij})$, $[\bar{\mathbf{O}}(i, j, \bar{\mathbf{H}})]_{i,j} = j \sin(\theta_O^{ij})$, $[\bar{\mathbf{O}}(i, j, \bar{\mathbf{H}})]_{j,i} = j \sin(\theta_O^{ij})$, $[\bar{\mathbf{O}}(i, j, \bar{\mathbf{H}})]_{j,j} = \cos(\theta_O^{ij})$ where

$$\theta_O^{ij} = \text{Atan}(\|\bar{\mathbf{h}}_i\|^2 - \|\bar{\mathbf{h}}_j\|^2, \langle \bar{\mathbf{h}}_i, \bar{\mathbf{h}}_j \rangle_I).$$

It is straightforward to show that the above two rotation matrices are unitary, i.e., $\bar{\mathbf{I}}(i, j, \bar{\mathbf{H}})^\dagger \bar{\mathbf{I}}(i, j, \bar{\mathbf{H}}) = \bar{\mathbf{O}}(i, j, \bar{\mathbf{H}})^\dagger \bar{\mathbf{O}}(i, j, \bar{\mathbf{H}}) = \mathbf{I}_{M_t}$. These two operations will affect only two columns i and j while leaving the rest of the matrix unchanged.

Our goal is to construct an M_t -by-two matrix $\bar{\mathbf{F}}_b$ which increases the minimum Euclidean distance $d_{min}^2(\bar{\mathbf{H}}_b, \bar{\mathbf{F}}_s^*)$ in (16) for $\bar{\mathbf{H}}_b = \bar{\mathbf{H}} \cdot \bar{\mathbf{F}}_b = [\bar{\mathbf{h}}_1^b \ \bar{\mathbf{h}}_2^b]$. In this paper, instead of directly constructing $\bar{\mathbf{F}}_b$, we first design an M_t -by- M_t matrix $\bar{\mathbf{F}}_B$ which increases $d_{min}^2(\bar{\mathbf{H}}_b, \bar{\mathbf{F}}_s^*)$ in (16), and then obtain $\bar{\mathbf{F}}_b$ as the M_t -by-two submatrix by taking the first and second columns from $\bar{\mathbf{F}}_B$. Here $\bar{\mathbf{H}}_b$ represents the M_r -by-two submatrix obtained by taking the first two columns from the matrix

$$\bar{\mathbf{H}}_B = \bar{\mathbf{H}} \cdot \bar{\mathbf{F}}_B = [\bar{\mathbf{h}}_1^b \ \bar{\mathbf{h}}_2^b \ \cdots \ \bar{\mathbf{h}}_{M_t}^b]. \quad (17)$$

Note that adopting this approach allows us to build an M_t -by-two matrix $\bar{\mathbf{F}}_b$ based on M_t -by- M_t rotation matrices $\bar{\mathbf{I}}(i, j, \bar{\mathbf{H}})$ and $\bar{\mathbf{O}}(i, j, \bar{\mathbf{H}})$.

We will increase the minimum Euclidean distance $d_{min}^2(\bar{\mathbf{H}}_b, \bar{\mathbf{F}}_s^*)$ by increasing the norm of columns $\bar{\mathbf{h}}_1^b$ and $\bar{\mathbf{h}}_2^b$ in (17). As shown in Equation (2), the norm of one column is maximized while the norm of the other column is minimized when orthogonality between the two columns is established. Using this observation, we can maximize the norm $\|\bar{\mathbf{h}}_1^b\|$

and $\|\bar{\mathbf{h}}_2^b\|$ by trying to make the column vectors $\bar{\mathbf{h}}_1^b$ and $\bar{\mathbf{h}}_2^b$ orthogonal to the other columns $\bar{\mathbf{h}}_k^b$ ($k \neq 1$ or 2). Although such an optimal precoding matrix $\bar{\mathbf{F}}_B$ can be obtained by utilizing the SVD of the channel matrix $\bar{\mathbf{H}}$, we employ the orthogonalization process of two vectors based on $\bar{\mathbf{I}}(i, j, \bar{\mathbf{H}})$ and $\bar{\mathbf{O}}(i, j, \bar{\mathbf{H}})$ as a constructive basis for the development of $\bar{\mathbf{F}}_B$ to avoid high computational complexity associated with the SVD operation.

For illustrative purposes, let us establish the inner and outer orthogonality between two complex vectors $\bar{\mathbf{v}}_1'$ and $\bar{\mathbf{v}}_2'$ in (2) by means of the inner and outer rotation transformations, respectively. Note that the inner rotation operation $\bar{\mathbf{I}}(\theta_I)$ in (11) can be used to force $\langle \bar{\mathbf{v}}_1', \bar{\mathbf{v}}_2' \rangle_R$ to zero, while the outer rotation $\bar{\mathbf{O}}(\theta_O)$ in (12) can be employed to annihilate the value of $\langle \bar{\mathbf{v}}_1', \bar{\mathbf{v}}_2' \rangle_I$. As a result, the established orthogonality increases the norm of $\bar{\mathbf{v}}_1'$. Substituting $\bar{\mathbf{P}}_o = \bar{\mathbf{I}}(\theta_I)$ in (2) yields

$$\begin{aligned} \|\bar{\mathbf{v}}_1'\|^2 &= \frac{\|\bar{\mathbf{v}}_1\|^2 + \|\bar{\mathbf{v}}_2\|^2}{2} \\ &+ \sqrt{\left(\frac{\|\bar{\mathbf{v}}_1\|^2 - \|\bar{\mathbf{v}}_2\|^2}{2}\right)^2 + \langle \bar{\mathbf{v}}_1, \bar{\mathbf{v}}_2 \rangle_R^2}. \end{aligned} \quad (18)$$

Similarly with $\bar{\mathbf{P}}_o = \bar{\mathbf{O}}(\theta_O)$, we have

$$\begin{aligned} \|\bar{\mathbf{v}}_1'\|^2 &= \frac{\|\bar{\mathbf{v}}_1\|^2 + \|\bar{\mathbf{v}}_2\|^2}{2} \\ &+ \sqrt{\left(\frac{\|\bar{\mathbf{v}}_1\|^2 - \|\bar{\mathbf{v}}_2\|^2}{2}\right)^2 + \langle \bar{\mathbf{v}}_1, \bar{\mathbf{v}}_2 \rangle_I^2}. \end{aligned} \quad (19)$$

Therefore, comparing (18) and (19), it is obvious that in order to maximize $\|\bar{\mathbf{v}}_1'\|^2$, we should choose $\bar{\mathbf{I}}(\theta_I)$ if $|\langle \bar{\mathbf{v}}_1, \bar{\mathbf{v}}_2 \rangle_R| \geq |\langle \bar{\mathbf{v}}_1, \bar{\mathbf{v}}_2 \rangle_I|$ for the beamforming process between two complex columns. Similarly we choose $\bar{\mathbf{O}}(\theta_O)$ if $|\langle \bar{\mathbf{v}}_1, \bar{\mathbf{v}}_2 \rangle_R| < |\langle \bar{\mathbf{v}}_1, \bar{\mathbf{v}}_2 \rangle_I|$. We notice that the inner rotation operation does not affect the value of $\langle \bar{\mathbf{v}}_1, \bar{\mathbf{v}}_2 \rangle_I$ (i.e., $\langle \bar{\mathbf{v}}_1', \bar{\mathbf{v}}_2' \rangle_I = \langle \bar{\mathbf{v}}_1, \bar{\mathbf{v}}_2 \rangle_I$), while the outer rotation leaves the value of $\langle \bar{\mathbf{v}}_1, \bar{\mathbf{v}}_2 \rangle_R$ unchanged (i.e., $\langle \bar{\mathbf{v}}_1', \bar{\mathbf{v}}_2' \rangle_R = \langle \bar{\mathbf{v}}_1, \bar{\mathbf{v}}_2 \rangle_R$). This means that inner orthogonality between columns pre-established in (11) remains unaffected by subsequent outer operations in (12). Considering this fact, we may achieve the complex orthogonality $\langle \bar{\mathbf{v}}_1', \bar{\mathbf{v}}_2' \rangle = 0$ with extra complexity by employing the inner rotation $\bar{\mathbf{I}}(\theta_I)$ and then applying the subsequent outer rotation $\bar{\mathbf{O}}(\theta_O)$. We notice that a compromise between complexity and performance needs to be made in designing $\bar{\mathbf{F}}_B$. Instead of pursuing complex orthogonality, in this paper we describe the beamforming transformation $\bar{\mathbf{F}}_B$ which can be realized with moderate complexity while maintaining a sufficient performance gain. Simulation results show that for the case of the complex orthogonality the performance improvement is marginal in spite of the increase in complexity. Thus, we consider the beamforming transformation as $\bar{\mathbf{F}}_B = \prod_{k=3}^{M_t} \bar{\mathbf{F}}_{B,k}$ where each component transformation $\bar{\mathbf{F}}_{B,k}$ employs only one of the rotation matrices $\bar{\mathbf{I}}(i, j, \bar{\mathbf{H}})$ and $\bar{\mathbf{O}}(i, j, \bar{\mathbf{H}})$. Specifically, with the aim of maximizing $d_{\min}^2(\bar{\mathbf{H}}_b, \bar{\mathbf{F}}_s^*)$, we apply the component transformation $\bar{\mathbf{F}}_{B,k} = \bar{\mathbf{F}}_{B,k}^1$ or $\bar{\mathbf{F}}_{B,k}^2$ depending on the current channel conditions, where $\bar{\mathbf{F}}_{B,k}^m$ represents

the rotation transformation to establish orthogonality between columns $\bar{\mathbf{h}}_m^b$ and $\bar{\mathbf{h}}_k^b$ (for $m = 1$ or 2 and $k = 3, 4, \dots, M_t$).

The algorithm for determining $\bar{\mathbf{F}}_B$ starts with an initialization process $\bar{\mathbf{H}}_B = \bar{\mathbf{H}}$ (see algorithm below). For each step, we determine the rotation transformations $\bar{\mathbf{F}}_{B,k}^1$ and $\bar{\mathbf{F}}_{B,k}^2$ on the pair of $(\bar{\mathbf{h}}_1^b, \bar{\mathbf{h}}_k^b)$ and $(\bar{\mathbf{h}}_2^b, \bar{\mathbf{h}}_k^b)$, respectively, and select the one that maximizes the minimum Euclidean distance. For the first step ($k = 3$), a rotation transformation $\bar{\mathbf{F}}_{B,3}^1$ on the pair of $(\bar{\mathbf{h}}_1^b, \bar{\mathbf{h}}_3^b)$ is made as follows. We compute $|\langle \bar{\mathbf{h}}_1^b, \bar{\mathbf{h}}_3^b \rangle|$ and $|\langle \bar{\mathbf{h}}_2^b, \bar{\mathbf{h}}_3^b \rangle|$ and choose $\bar{\mathbf{F}}_{B,3}^1 = \bar{\mathbf{I}}(1, 3, \bar{\mathbf{H}}_B)$ if $|\langle \bar{\mathbf{h}}_1^b, \bar{\mathbf{h}}_3^b \rangle_R| \geq |\langle \bar{\mathbf{h}}_2^b, \bar{\mathbf{h}}_3^b \rangle_I|$, otherwise choose $\bar{\mathbf{F}}_{B,3}^1 = \bar{\mathbf{O}}(1, 3, \bar{\mathbf{H}}_B)$. Define the intermediate channel matrix as $\bar{\mathbf{H}}_B^m = \bar{\mathbf{H}}_B \bar{\mathbf{F}}_{B,3}^m$ ($m = 1, 2$) and $\bar{\mathbf{H}}_B^m$ is given as the M_r -by-two matrix with the first two columns of $\bar{\mathbf{H}}_B^m$. Then, we determine the optimal mode $\bar{\mathbf{F}}_{s,1}^*$ from (16) as $\bar{\mathbf{F}}_{s,1}^* = \arg \max_{\bar{\mathbf{F}}_s \in \mathcal{F}_U} d_{\min}^2(\bar{\mathbf{H}}_b^1, \bar{\mathbf{F}}_s)$ (for the intermediate channel matrix $\bar{\mathbf{H}}_B^1 = \bar{\mathbf{H}}_B \bar{\mathbf{F}}_{B,3}^1$) and denote the corresponding minimum Euclidean distance as $D_3^1 = d_{\min}^2(\bar{\mathbf{H}}_b^1, \bar{\mathbf{F}}_{s,1}^*)$.

In a similar way, we determine the rotation transformation $\bar{\mathbf{F}}_{B,3}^2$ on the pair of $(\bar{\mathbf{h}}_2^b, \bar{\mathbf{h}}_3^b)$ by comparing $|\langle \bar{\mathbf{h}}_2^b, \bar{\mathbf{h}}_3^b \rangle_R|$ and $|\langle \bar{\mathbf{h}}_1^b, \bar{\mathbf{h}}_3^b \rangle_I|$ and then evaluate $D_3^2 = d_{\min}^2(\bar{\mathbf{H}}_b^2, \bar{\mathbf{F}}_{s,2}^*)$ by computing $\bar{\mathbf{H}}_B^2 = \bar{\mathbf{H}}_B \bar{\mathbf{F}}_{B,3}^2$. Finally, we obtain the first component transformation $\bar{\mathbf{F}}_{B,3} = \bar{\mathbf{F}}_{B,3}^{m_3}$ where $m_3 = \arg \max_{m \in \{1,2\}} D_3^m$ and update as $\bar{\mathbf{H}}_B = \bar{\mathbf{H}}_B^{m_3}$.

At each subsequent step $k = 4, \dots, M_t$, we determine the component transformation $\bar{\mathbf{F}}_{B,k} = \bar{\mathbf{F}}_{B,k}^{m_k}$ at the same way. To summarize, we perform $M_t - 2$ successive transformations $\bar{\mathbf{F}}_{B,k}$ on the column pairs $(\bar{\mathbf{h}}_{m_k}^b, \bar{\mathbf{h}}_k^b)$ ($k = 3, 4, \dots, M_t$) where m_k is either 1 or 2 depending on the minimum distance D_k^m . The whole algorithm can be described as follows:

We note again that the beamforming transformation $\bar{\mathbf{F}}_b$ is obtained as the M_t -by-two submatrix by taking the first two columns from $\bar{\mathbf{F}}_B = \prod_{k=3}^{M_t} \bar{\mathbf{F}}_{B,k}$. It is also important to note that the orthogonalization transformation $\bar{\mathbf{F}}_s$ is given by the optimal mode for $k = M_t$ (i.e., $\bar{\mathbf{F}}_s = \bar{\mathbf{F}}_{s,m_k}^*$ with $k = M_t$). This approach can be applied for any number of receive antennas greater than or equal to two.

Now we will briefly address the computational complexity issue. The main computational cost for each step $k = 3, \dots, M_t$ can be assessed as follows:

- 1) When determining the rotation transformation $\bar{\mathbf{F}}_{B,k}^1$ and $\bar{\mathbf{F}}_{B,k}^2$, we need the computations of $\|\bar{\mathbf{h}}_1^b\|$, $\|\bar{\mathbf{h}}_2^b\|$, $\|\bar{\mathbf{h}}_k^b\|$, $\langle \bar{\mathbf{h}}_1^b, \bar{\mathbf{h}}_k^b \rangle$, and $\langle \bar{\mathbf{h}}_2^b, \bar{\mathbf{h}}_k^b \rangle$. We notice that for $k \geq 4$ the norm values of $\|\bar{\mathbf{h}}_1^b\|$ and $\|\bar{\mathbf{h}}_2^b\|$ are given by Equations (18) and (19) during the computation of $\bar{\mathbf{F}}_{s,m}^*$ at the preceding step.
- 2) The computation complexity of $\bar{\mathbf{H}}_B^m = \bar{\mathbf{H}}_B \bar{\mathbf{F}}_{B,k}^m$ is equivalent to that of the product of an M_r -by-two complex matrix and a two-by-one real vector since only the m -th column of $\bar{\mathbf{H}}_B^m$ (for $m = 1$ or 2) needs to be evaluated and $\bar{\mathbf{F}}_{B,k}^m$ (which is either $\bar{\mathbf{I}}(m, k, \bar{\mathbf{H}}_B)$ or $\bar{\mathbf{O}}(m, k, \bar{\mathbf{H}}_B)$) has

```

1:  $\overline{\mathbf{H}}_B = \overline{\mathbf{H}}$ 
2: for  $k = 3 : M_t$ 
3:   for  $m = 1 : 2$ 
4:     if  $\left| \left\langle \overline{\mathbf{h}}_m^b, \overline{\mathbf{h}}_k^b \right\rangle_R \right| \geq \left| \left\langle \overline{\mathbf{h}}_m^b, \overline{\mathbf{h}}_k^b \right\rangle_I \right|$ 
5:        $\overline{\mathbf{F}}_{B,k}^m = \overline{\mathbf{I}}(m, k, \overline{\mathbf{H}}_B)$ 
6:     else
7:        $\overline{\mathbf{F}}_{B,k}^m = \overline{\mathbf{O}}(m, k, \overline{\mathbf{H}}_B)$ 
8:     end
9:      $\overline{\mathbf{H}}_B^m = \overline{\mathbf{H}}_B \overline{\mathbf{F}}_{B,k}^m$ 
10:     $\overline{\mathbf{F}}_{s,m}^* = \arg \max_{\overline{\mathbf{F}}_s \in \mathcal{F}_U} d_{min}^2 \left( \overline{\mathbf{H}}_B^m, \overline{\mathbf{F}}_s \right)$ 
11:     $D_k^m = d_{min}^2 \left( \overline{\mathbf{H}}_B^m, \overline{\mathbf{F}}_{s,m}^* \right)$ 
12:  end
13:   $m_k = \arg \max_{m \in \{1,2\}} D_k^m$ 
14:   $\overline{\mathbf{F}}_{B,k} = \overline{\mathbf{F}}_{B,k}^{m_k}$  and  $\overline{\mathbf{H}}_B = \overline{\mathbf{H}}_B^{m_k}$ 
15: end
16:  $\overline{\mathbf{F}}_B = \prod_{k=3}^{M_t} \overline{\mathbf{F}}_{B,k}$ 
    
```

only four pure real and pure imaginary non-zero elements plus ones on the diagonal.

- 3) When determining the matrix $\overline{\mathbf{F}}_{s,m}^*$ for $\overline{\mathbf{H}}_B^m = \begin{bmatrix} \overline{\mathbf{h}}_1^{b,m} & \overline{\mathbf{h}}_2^{b,m} \end{bmatrix}$, we need the values of $\|\overline{\mathbf{h}}_1^{b,m}\|$, $\|\overline{\mathbf{h}}_2^{b,m}\|$ and $\left\langle \overline{\mathbf{h}}_1^{b,m}, \overline{\mathbf{h}}_2^{b,m} \right\rangle$ in computing three rotation matrices $\overline{\mathbf{F}}_s$ of set \mathcal{F}_U . Note that $\|\overline{\mathbf{h}}_1^{b,m}\|$ and $\|\overline{\mathbf{h}}_2^{b,m}\|$ are given by Equations (18) or (19) according to $\overline{\mathbf{F}}_{B,k}^m$ in the update $\overline{\mathbf{H}}_B^m = \overline{\mathbf{H}}_B \overline{\mathbf{F}}_{B,k}^m$. The computation complexity of $d_{min}^2 \left(\overline{\mathbf{H}}_B^m, \overline{\mathbf{F}}_s \right)$ in Equations (14) and (15) for each $\overline{\mathbf{F}}_s$ consists of the product of an M_r -by-two complex matrix and a two-by-two real matrix, $S(M_c)$ products of a $2M_r$ -by-two real matrix and a two-by-one real vector, and $S(M_c)$ inner products between $2M_r$ -dimensional real vectors. Here $S(M_c)$ denotes the size of the search set in the computation of the minimum distance for M_c -QAM constellation.
- 4) The computation complexity of $\overline{\mathbf{F}}_B = \prod_{k=3}^{M_t} \overline{\mathbf{F}}_{B,k}$ is negligible compared to the above three cases since each transformation $\overline{\mathbf{F}}_{B,k}$ has only four pure real or imaginary elements considered in matrix products and only the first two columns of $\overline{\mathbf{F}}_B$ are to be evaluated.

In summary, for $M_t > 2$, the proposed scheme requires $(36M_t \cdot S(M_c) + 74M_t - 72S(M_c) - 144)M_r$ real multiplications for each channel realization. It is shown in [21] that the size of the search set in (14) and (15) is only $S(M_c) = 2$ and 5 for $M_c = 4$ and 16, respectively, which indicates that the complexity of the proposed method increases only linearly with the number of transmit and receive antennas. We notice that in the application of the proposed method, we can evaluate rotation matrices without computing the angles. For example, $\cos(\theta_I)$ and $\sin(\theta_I)$ for the inner rotation matrix $\overline{\mathbf{I}}(\theta_I)$ in (11)

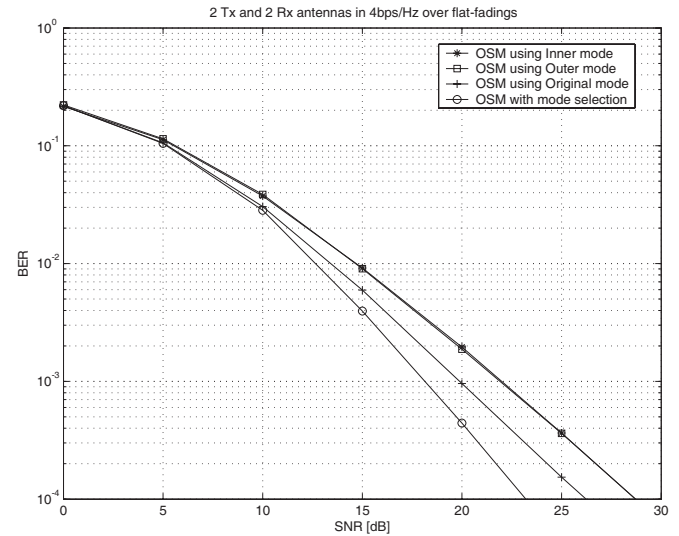


Fig. 2. Bit-error-rate performance comparison for the OSM transmission with and without mode selection.

can be evaluated as follows: $\cos(\theta_I) = \frac{1}{\sqrt{t^2+1}}$ and $\sin(\theta_I) = t \cos(\theta_I)$ where $t = \frac{x - \sqrt{x^2+4y^2}}{2y}$ with $x = \|\overline{\mathbf{h}}_1^b\|^2 - \|\overline{\mathbf{h}}_2^b\|^2$ and $y = \left\langle \overline{\mathbf{h}}_1^b, \overline{\mathbf{h}}_2^b \right\rangle_R$.

In contrast, for the SVD-based transmission presented in [16], [17] and [18] we need to compute M dominant right singular vectors of the channel matrix. The iterative power method is known to be particularly suited for computing the dominant singular vectors of a matrix [19], which requires $(8M_tM_r + 4M_t + 4M_r)MN_i + 4M_tM_r(M-1)$ real multiplications in the SVD operation of an $M_r \times M_t$ matrix, where N_i is the number of iterations in the power method. In the simulation section, we will demonstrate that compared to the SVD schemes based on the power method, the proposed scheme achieves better performance with reduced complexity.

It is also worthy of note that other variations of this algorithm are conceivable depending on a trade-off between performance and complexity. For example, we can further improve the performance of the proposed scheme by choosing two columns of the channel matrix $\overline{\mathbf{H}}$ as described in [20] and constructing $\overline{\mathbf{F}}_B$ to maximize the distance criterion (16) for the selected two columns.

V. SIMULATION RESULTS

In this section, we present simulation results to demonstrate the efficacy of the proposed two step approach for closed-loop MIMO systems in flat fading channels. We assume that the elements of the MIMO channel matrix $\overline{\mathbf{H}}$ are obtained from an independent and identically distributed (i.i.d.) complex Gaussian distribution. We also assume that the number of transmitted spatial streams is two ($M = 2$) for all simulations. Various closed-loop MIMO schemes are evaluated in terms of the BER performance as a function of the average SNR in dB.

We first present the simulation results of the OSM mode selection method based on the minimum Euclidean distance described in (16) which determines the optimal OSM mode for each channel realization. In Fig. 2, we compare the BER

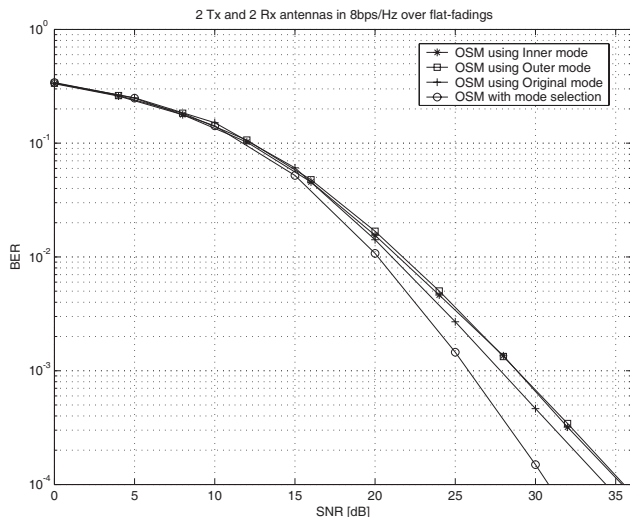


Fig. 3. Bit-error-rate performance comparison for the OSM transmission with and without mode selection.

performance of various OSM modes for a MIMO system with two transmit and two receive antennas using 4QAM. Our mode selection offers 2.5 dB and 5 dB SNR gains over the original mode OSM proposed in [21] and the fixed inner or outer mode OSM, respectively, at a BER of 10^{-4} .

Fig. 3 illustrates the performance comparison for the same antenna configuration with 16QAM. The simulation results exhibit the same trend as in Fig. 2 except that the performance gap between the original mode OSM and the inner or outer mode OSM decreases as the constellation size grows. The proposed selection scheme still provides a 5 dB gain over the fixed inner or outer mode. These simulation results show that we can achieve a significant performance gain by properly choosing the OSM mode based on the proposed selection criterion for each channel realization.

For the simulation results in Figs. 4 and 5, we will compare the following systems:

- *Optimal Unitary Precoding (OUP)*: A unitary matrix based on SVD of the MIMO channel is applied to diagonalize the channel matrix [15].
- *Optimal Linear Precoding (OLP)*: Jointly optimized linear precoder and decoder are applied based on the minimum mean square error (MMSE) criterion [16] which minimizes the sum of the mean square errors (MSEs) of all subchannels.

For comparison purposes, we also consider the performance of ML detection algorithm in (open-loop) MIMO systems with M_t transmit and M_r receive antennas (denoted by " $M_t \times M_r$ MIMO with MLD"), where the number of the search candidates for the ML detection is $M_c^{M_t}$ without any precoding.

In Figs. 4 and 5, we depict the BER comparison of the proposed precoding and two SVD-based precodings with $M_r = 2$ and 4QAM. We remark that for the two receive antenna case the SVD solution of a MIMO channel can be obtained in a closed form without numerical problems. For the $M_t = 3$ case presented in Fig. 4, we can see that at a BER of 10^{-4} the proposed precoding provides a 7.5 dB gain over the 2×2 MIMO with MLD scheme. More importantly,

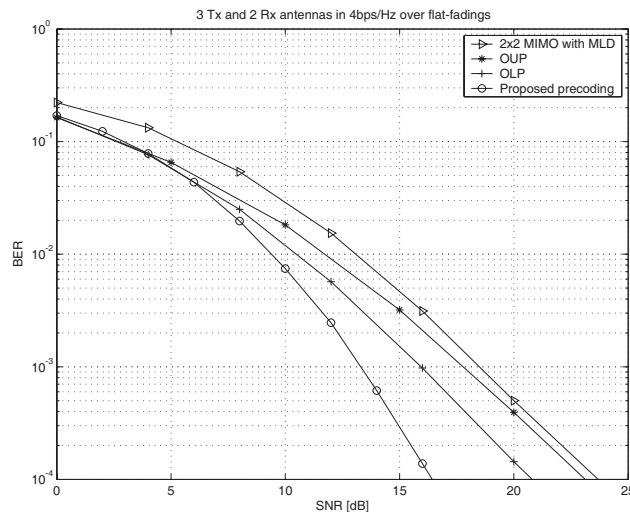


Fig. 4. Bit-error-rate performance comparison between the proposed scheme, OUP and OLP.

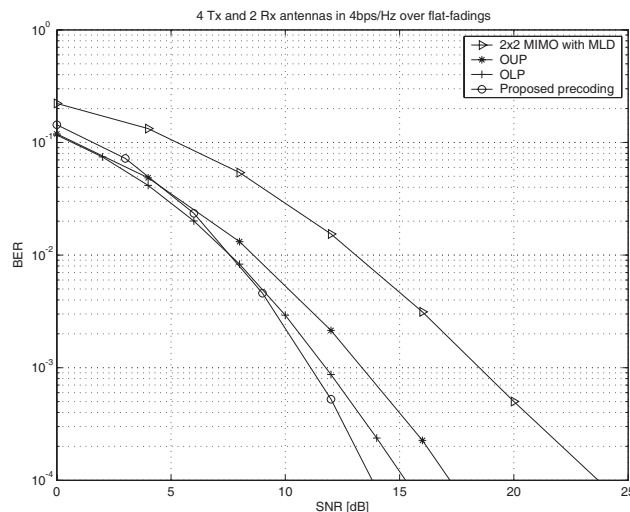


Fig. 5. Bit-error-rate performance comparison between the proposed scheme, OUP and OLP.

Fig. 4 shows that the performance of the proposed precoding is 7 dB and 4.5 dB better than the OUP and OLP, respectively. As the number of transmit antennas increases to 4 in Fig. 5, the performance gain over the 2×2 ML case grows up to 10 dB at a BER of 10^{-4} . This figure also shows that the proposed two step precoding outperforms both the OUP and OLP by 3.5 dB and 1.5 dB, respectively. In the case of these SVD-based methods, data streams assigned to weaker eigen modes dominate the overall system performance since the weaker subchannels are more prone to errors. This causes the OUP and OLP methods to perform worse than the proposed two step precoding.

In order to improve the BER performance of the OLP method, we can further apply the rotation matrix to the OLP so that the MSEs become identical as suggested by [18], and this will be denoted by "*ARITH-BER*". As the rotation matrix is applied to the OLP, the orthogonality among MIMO spatial subchannels is lost. Thus, to mitigate intersymbol interference and to allow for a simple receiver structure we use the optimal

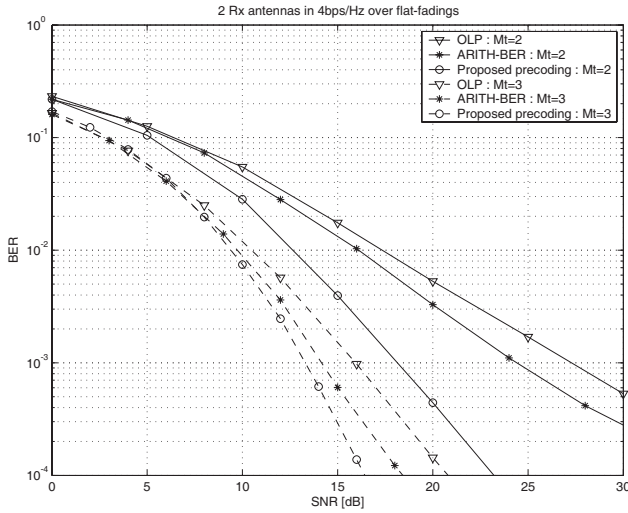


Fig. 6. Bit-error-rate performance comparison for two/three transmit and two receive antenna.

MSE receive matrix presented in [18]. While not included in this paper due to space limitation, we have witnessed that when combined with the symbol rotation method in [18] the proposed scheme can also achieve up to 1 dB gain without additional complexity.

Fig. 6 compares the performance of the proposed method and ARITH-BER with 4QAM. In this figure, the number of receive antennas is fixed to 2, while the number of transmit antennas is set to 2 and 3. Fig. 6 shows that the proposed method outperforms the ARITH-BER method by more than 6 dB at a BER of 10^{-3} for $M_t = 2$. This result can be explained as follows. The ARITH-BER algorithm assumes a symbol-by-symbol detection, whereas, as can be seen in (5), we perform joint detection of the two transmitted signals. Remember that the actual detection is still done at the same computational complexity as symbol-by-symbol detection due to the decoupling between real and imaginary parts. The performance gap between the proposed and ARITH-BER methods reduces to approximately 2 dB at a BER of 10^{-4} as M_t increases to 3. The benefit of the increased number of antennas is more pronounced for the ARITH-BER method than our scheme since the ARITH-BER better exploits the increased available diversity by performing the full SVD decomposition of a transfer matrix, allocating the total transmit power to spatial subchannels and applying a pre-rotation of the data symbols at the transmitter. Meanwhile, the proposed precoding algorithm becomes more attractive than ARITH-BER in terms of computational complexity.

Finally, in Fig. 7, the BER performance of the SVD scheme based on the iterative power method is simulated for 3×3 MIMO systems. Note that with a finite number of iterations the SVD-based schemes cannot completely decompose the MIMO channel into parallel independent subchannels. In this case, there exist no simple analytical solutions for power allocation and thus only the OUP scheme is considered in the simulation. We have used an MMSE receiver in order to handle the subchannel interference due to incomplete channel decomposition. Through computer simulations, we found that

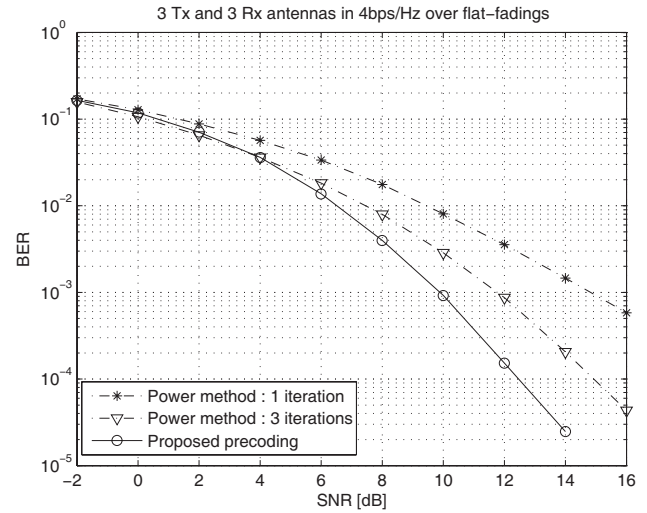


Fig. 7. Comparison between the proposed scheme and the SVD scheme based on the power method.

$N_i = 3$ iterations are required for the power method to achieve the BER performance of the case with perfect right singular vectors for this antenna configuration. Fig. 7 shows that the proposed scheme outperforms the conventional SVD-based scheme with reduced complexity as the proposed scheme requires 450 multiplications, while the power method needs 612 multiplications.

VI. CONCLUSION

In this paper, we have proposed a new MIMO transmission technique which divides the precoding process into two steps: orthogonalization transformation and beamforming transformation. The orthogonalization and beamforming transformations are developed to increase the minimum Euclidean distance between two different received signal vectors. Meanwhile, we have used three rotation matrices to induce inner and outer orthogonality between two column vectors. The established orthogonality provides two important properties. First, a simple ML decoder is made possible at the receiver to decode two transmitted signals. Second, the search complexity of the minimum Euclidean distance between received signal vectors is substantially reduced. Because of the intractable nature of finding closed-form expressions for the average BER for the proposed system, numerical Monte-Carlo simulation results are provided to evaluate the proposed method. Simulation results show that the proposed precoding achieves a performance gain over the SVD-based precodings while requiring lower complexity.

Due to practical limitations on the number of antennas for MIMO systems, we have considered spatial multiplexing systems transmitting two independent data streams in this paper. The concept of the proposed two-step precoding strategy can be extended to more than two data streams ($M > 2$). The analysis of the diversity and array gains achievable with the proposed system is also an interesting topic for future work.

REFERENCES

- [1] G. J. Foschini and M. Gans, "On limits of wireless communications in a fading environment when using multiple antennas," *IEEE Wireless Personal Commun.*, vol. 6, pp. 311–335, Mar. 1998.
- [2] I. E. Telatar, "Capacity of multi-antenna Gaussian channels," *Eur. Trans. Telecommun.*, vol. 10, pp. 585–595, Nov. 1999.
- [3] L. Zheng and D. N. C. Tse, "Diversity and multiplexing: a fundamental tradeoff in multiple-antennas channels," *IEEE Trans. Inform. Theory*, vol. 49, pp. 1073–1096, May 2003.
- [4] E. Sengul, E. Akay, and E. Ayanoglu, "Diversity analysis of single and multiple beamforming," *IEEE Trans. Commun.*, vol. 54, pp. 990–993, June 2006.
- [5] D. Gesbert, M. Shafi, D. Shan Shiu, P. Smith, and A. Naguib, "From theory to practice: an overview of MIMO space-time coded wireless systems," *IEEE J. Select. Areas Commun.*, vol. 21, pp. 281–302, Apr. 2003.
- [6] S. M. Alamouti, "A simple transmit diversity scheme for wireless communications," *IEEE J. Select. Areas Commun.*, pp. 1451–1458, Oct. 1998.
- [7] V. Tarokh, N. Seshadri, and A. R. Calderbank, "Space-time codes for high data rate wireless communication: performance criterion and code construction," *IEEE Trans. Inform. Theory*, vol. 44, pp. 744–765, Mar. 1998.
- [8] H. Lee, J. Cho, J.-K. Kim, and I. Lee, "An efficient decoding algorithm for STBC with multidimensional rotated constellations," in *Proc. IEEE ICC*, June 2006.
- [9] P. W. Wolniansky, G. J. Foschini, G. D. Golden, and R. A. Valenzuela, "V-BLAST: an architecture for realizing very high data rates over the rich-scattering wireless channel," in *Proc. URSI International Symp. Signals, Syst. Electronics*, Sept. 1998, pp. 295–300.
- [10] H. Lee, B. Lee, and I. Lee, "Iterative detection and decoding with an improved V-BLAST for MIMO-OFDM systems," *IEEE J. Select. Areas Commun.*, vol. 24, pp. 504–513, Mar. 2006.
- [11] H. Lee and I. Lee, "New approach for error compensation in coded V-BLAST OFDM systems," *IEEE Trans. Commun.*, vol. 55, pp. 345–355, Feb. 2007.
- [12] A. J. Goldsmith and P. P. Varaiya, "Capacity of fading channels with channel side information," *IEEE Trans. Inform. Theory*, vol. 43, pp. 1986–1992, Nov. 1997.
- [13] A. J. Goldsmith, S. A. Jafar, N. J. Jindal, and S. Vishwanath, "Capacity limits of MIMO channels," *IEEE J. Select. Areas Commun.*, vol. 21, pp. 684–702, June 2003.
- [14] G. G. Raleigh and J. M. Cioffi, "Spatio-temporal coding for wireless communication," *IEEE Trans. Commun.*, vol. 46, pp. 357–366, Mar. 1998.
- [15] J. B. Andersen, "Array gain and capacity for known random channels with multiple element arrays at both ends," *IEEE J. Select. Areas Commun.*, vol. 18, pp. 2172–2178, Nov. 2000.
- [16] H. Sampath, P. Stoica, and A. Paulraj, "Generalized linear precoder and decoder design for MIMO channels using the weighted MMSE criterion," *IEEE Trans. Commun.*, vol. 49, pp. 2198–2206, Dec. 2001.
- [17] A. Scaglione, P. Stoica, S. Barbarossa, G. B. Giannakis, and H. Sampath, "Optimal designs for space-time linear precoders and decoders," *IEEE Trans. Signal Processing*, vol. 50, pp. 1051–1064, May 2002.
- [18] D. P. Palomar, J. M. Cioffi, and M. A. Lagunas, "Joint Tx-Rx beamforming design for multicarrier MIMO channels: a unified framework for convex optimization," *IEEE Trans. Signal Processing*, vol. 51, pp. 2381–2401, Sept. 2003.
- [19] G. H. Golub and C. F. V. Loan, *Matrix Computations*, 3rd ed. Baltimore and London: The Johns Hopkins University Press, 1996.
- [20] H. Lee, S.-H. Park, and I. Lee, "Orthogonalized spatial multiplexing for MIMO systems," in *Proc. IEEE VTC-Fall*, Sept. 2006.
- [21] H. Lee, S.-H. Park, and I. Lee, "Orthogonalized spatial multiplexing for closed-loop MIMO systems," *IEEE Trans. Commun.*, vol. 55, pp. 1044–1052, May 2007.
- [22] H. Lee, S.-H. Park, and I. Lee, "A new MIMO beamforming technique based on rotation transformation," in *Proc. IEEE ICC*, June 2007.
- [23] R. W. Heath and A. J. Paulraj, "Antenna selection for spatial multiplexing systems based on minimum error rate," in *Proc. IEEE ICC*, June 2001, vol. 7, pp. 2276–2280.
- [24] P. A. Dighe, R. K. Malik, and S. S. Jamuar, "Analysis of transmit-receive diversity in Rayleigh fading," *IEEE Trans. Commun.*, vol. 51, pp. 694–703, Apr. 2003.
- [25] J. C. Nash, "A one-sided transformation method for the singular value decomposition and algebraic eigenproblem," *Computer J.*, vol. 18, no. 1, pp. 74–76, Feb. 1975.
- [26] A. M. Chan and I. Lee, "A new reduced-complexity sphere decoder for multiple antenna systems," in *Proc. IEEE ICC*, Apr. 2002, pp. 460–464.
- [27] H. Lee, S. Park, and I. Lee, "Transmit beamforming method based on maximum-norm combining for MIMO systems," *IEEE Trans. Wireless Commun.*, to be published.



Heunchul Lee (S'04-M'08) received the B.S., M.S., and Ph.D. degrees in electrical engineering from Korea University, Seoul, Korea, in 2003, 2005, and 2008, respectively. From February 2008 to October 2008 he was a Post-doctoral Fellow under the Brain Korea 21 Program at the same university. Since November 2008 he has been with the Department of Electrical Engineering at Stanford University, where he is currently a Post-doctoral Scholar. During the winter of 2006, he worked as an intern at Beceem Communications, Santa Clara, CA, USA.

His research interests are in communication theory and signal processing for wireless communications, including MIMO-OFDM systems and multi-user MIMO wireless networks. Dr. Lee received the Best Paper Award at the 12th Asia-Pacific conference on Communications, and the IEEE Seoul Section Student Paper Contest award, both in 2006. In addition, he was awarded the Bronze Prize in the 2007 Samsung Humantech Paper Contest in February 2008.



Seokhwan Park (S'05) received the B.S. and M.S. degrees in electrical engineering from Korea University, Seoul, Korea, in 2005 and 2007, where he is currently working toward the Ph.D. degree in the School of Electrical Engineering. His research interests include signal processing techniques for MIMO-OFDM systems. He has received the Best Paper Award at the 12th Asia-Pacific conference on communications, and the IEEE Seoul Section Student Paper Contest.



Inkyu Lee (S'92-M'95-SM'01) was born in Seoul, Korea in 1967. He received the B.S. degree (Hon.) in control and instrumentation engineering from Seoul National University, Seoul, Korea in 1990, and the M.S. and Ph.D. degrees in electrical engineering from Stanford University in 1992 and 1995, respectively. From 1991 to 1995, he was a Research Assistant at the Information Systems Laboratory, Stanford University. From 1995 to 2001, he was a Member of Technical Staff at Bell Laboratories, Lucent Technologies, where he studied high-speed

wireless system design. He later worked for Agere Systems (formerly the Microelectronics Group of Lucent Technologies), Murray Hill, NJ, as a Distinguished Member of Technical Staff from 2001 to 2002. In September 2002, he joined the faculty of Korea University, Seoul, Korea, where he is currently a Professor in the School of Electrical Engineering. He has published over 40 IEEE journal papers, and has 30 U.S. patents granted or pending. His research interests include digital communications, signal processing, and coding techniques applied to wireless systems with an emphasis on MIMO-OFDM. Dr. Lee currently serves as an Associate Editor for the IEEE TRANSACTIONS ON COMMUNICATIONS and the IEEE TRANSACTIONS ON WIRELESS COMMUNICATIONS. Also, he has been a Chief Guest Editor for the IEEE JOURNAL ON SELECTED AREAS IN COMMUNICATIONS (Special Issue on 4G Wireless Systems). He received the IT Young Engineer Award as the IEEE/IEEK joint award and the APCC Best Paper Award in 2006.